Chemistry & Biology, Vol. 9, 647–654, May, 2002, ©2002 Elsevier Science Ltd. All rights reserved. PII S1074-5521(02)00140-0

Toward the Synthesis of Artificial Proteins: The Discovery of an Amphiphilic Helical Peptoid Assembly

Timothy S. Burkoth,[1,2] Eric Beausoleil,[2] Surinder Kaur,[2] Dahzi Tang,[2] Fred E. Cohen,[1,3] and Ronald N. Zuckermann[2,3]

[1]Departments of Cellular and Molecular Pharmacology
University of California, San Francisco
San Francisco, California 94143
[2]Chiron Corporation
4560 Horton Street
Emeryville, California 94608

Summary

While nature exploits folded biopolymers to achieve molecular recognition and catalysis, comparable abiological heteropolymer systems have been difficult to create. We synthesized and identified abiological peptoid heteroploymers capable of binding a dye. Using combinatorial synthesis, we constructed a library of 3400 amphiphilic 15-mer peptoids on an ultra-high-capacity beaded support. Individual macrobeads, each containing a single peptoid sequence, were arrayed into plates, cleaved, and screened in aqueous solution to locate dye binding heteropolymer assemblies. Resynthesis and characterization demonstrated the formation of defined helical assemblies as judged by size-exclusion chromatography, circular dichroism, and analytical ultracentrifugation. Inspired by nature's process of sequence variation and natural selection, we identified rare abiological sequence-specific heteropolymers that begin to mimic the structure and functional properties of their biological counterparts.

Introduction

A major long-term goal of chemists and chemical engineers is to design low-cost and stable synthetic materials that display specific, high-affinity molecular recognition comparable to that of proteins and RNA. A variety of homo- and heteropolymer chemistries have fallen short of this goal owing to our limited understanding of molecular design principles coupled with substantial synthetic limitations. Clearly, nature has created a myriad of functionally specialized nanostructures using a limited set of monomers, a robust linking chemistry, and weak noncovalent interactions. Poly α amino acids and RNA form limited self-assembling structures to create binding and catalytic sites. For water-soluble globular proteins, the hydrophobic effect overcomes the conformational entropy of an unfolded polypeptide chain to yield a monomeric or oligomeric folded state with a distinct and often unique structure. Folding domains are typically 50–200 residues in length and utilize a specific sequence of side chains to encode tertiary structures enriched in secondary structure with hydrophobic cores that are shielded from solvent by a predominately hydrophilic surface [1]. Folded biological heteropolymeric systems that carry out specific functions are identified through nature's evolutionary process, utilizing efficient monomer coupling strategies (ribosomes, RNA polymerase), selection (competitive advantage), and a mechanism for resynthesis of the best sequences (DNA encoding a gene). We have exploited bioorganic and biophysical analogs of these processes and identified abiological heteropolymers that self-assemble to create a binding site for a hydrophobic small molecule dye.

To achieve this goal, we developed methods for efficient modular synthesis of *N*-substituted glycine heteropolymers that facilitate both side chain diversity and local secondary structure. A variety of other nonnatural polymers have been synthesized with many of these characteristics [2–7] with the goal of stable tertiary structure formation [8] and complex function. However, many are deficient in one or more key areas, such as poor coupling efficiency or limited monomer diversity. By contrast, peptoids are constructed in a stepwise manner by a solid phase submonomer method, yielding monodisperse sequence-specific heteropolymers up to 48 residues in length [9]. The robust chemistry can accommodate a variety of chemically diverse side chains ($>$100 monomers) and the use of combinatorial synthetic methodologies. Furthermore, peptoids with *N*-α chiral, aromatic side chains can fold into a repeating helical structure reminiscent of the polyproline type I helix [10]. Since these oligomers had limited water solubility, we needed to supplement them with additional chiral hydrophilic residues. We therefore included a series of additional monomers based on a substituted propanamide side chain that retain the chiral methyl group on the α carbon but replace the aromatic group with a series of simple substituted carboxamides [11].

Within nature, mutation is a source of sequence variation, and individual cells provide a forum for synthesizing, testing, and selecting polypeptide sequences with functional properties without explicit regard for structure [12]. In our approach, a diverse combinatorial library of amphiphilic 15-mer peptoids was prepared, and each sequence variant was physically compartmentalized by placing a single macrobead containing 20 nmol of synthetic material into a single well of a 96-well plate. Under aqueous conditions, the putative amphiphilic helix could multimerize by noncovalent association to form a helical assembly, thus creating a hydrophobic pocket capable of binding a ligand. The function we sought was efficient binding of 1-analinonaphthalene-8-sulfonate (1,8-ANS) to the hydrophobic pocket. When free in aqueous solution, 1,8-ANS exhibits little fluorescence, but when bound specifically [13] or nonspecifically [14, 15] in a hydrophobic environment, the dye exhibits strong fluorescence at 460 nm. This provides the basis for a convenient, highly sensitive, high-throughput screen for detecting the formation of a binding pocket. We report here the synthesis and characterization of a diverse

[3]Correspondence: cohen@cgl.ucsf.edu (F.E.C.), ron_zuckermann@chiron.com (R.N.Z.)

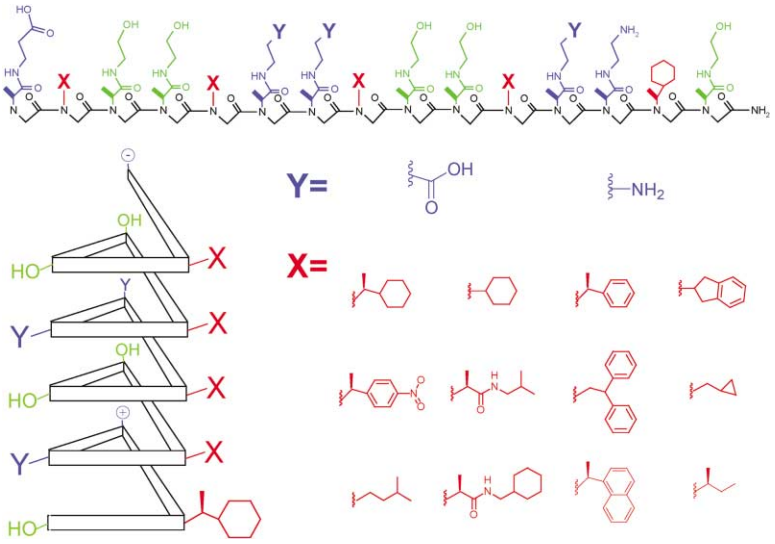

Figure 1. The 15-mer Amphiphilic Peptoid Sequence with a 3-Fold Periodicity Used as the Combinatorial Library Scaffold

A minimal set of helix-inducing ionic (blue) and polar nonionic (green) side chains were used. An assortment of hydrophobic side chains (red, indicated with an X) were incorporated every third residue. Hydrophilic residues were placed at ten positions within the sequence (seven fixed and three variable). The fixed polar positions allowed for a uniform degree of hydrophilicity and a reasonable P_i for every member of the library. The three variable positions (indicated with a Y) were either a cationic or anionic side chain and were used to explore potential interhelical electrostatic interactions. The first three residues at the C-terminal amide were kept constant to standardize potential end-capping interactions and help facilitate MS/MS sequencing.

combinatorial library used to identify peptoid sequences that self-associate and mimic some of the properties of proteins.

Results and Discussion

The design of the polypeptoid library for this study reflects compromises among synthetic accessibility, diversity of side chain functionalities, and screening and characterization capacity. Sequences of 15 residues in length with side chains chosen from a set of 15 different monomers were used in the library design (Figure 1). Previous structural studies showed that a chiral peptoid oligomer with S stereochemistry at the side chain carbon α to the backbone nitrogen has a helical shape with a right-handed helical twist. The amide bonds are all *cis* with the helix exhibiting a 3-fold periodicity and a pitch of $\sim$6 Å, where every third residue is directly aligned parallel to the helix axis [10]. As a general design motif, a 3-fold repeating pattern of hydrophobic and hydrophilic side chains was chosen to promote an amphiphilic helix. A high percentage of chiral side chains were introduced to stabilize the helix [16]. Moreover, a 15-residue peptoid helix has a length comparable to the α helices observed in helical bundle proteins [17]. The hydrophilic side chains for the library included an amine, an alcohol, and an acid functional group within the L-alanine *N′*-substituted amide monomer. These side chains represented a minimal, chemically diverse set of monomers, analogous to lysine, glutamic acid, and serine. Since hydrophobic forces dominate protein folding, 12 different hydrophobic monomers were introduced at four different positions within the 15-mer. A variety of different chiral, achiral, branched, cyclic, aromatic, and aliphatic side chains with varying degrees of hydrophobicity were used to explore the requirements for interior side chain packing and the magnitude of the hydrophobic effect required to form a stable multimer.

A mix-and-split combinatorial library synthetic strategy was used to explore a diverse molecular sequence space. The library consisted of 165,888 unique sequences, with approximately 18,000 (11%) compounds actually synthesized on ultra-high-capacity beads (macrobeads) using a robotic library synthesizer. The average synthetic yield of representative 15-mers from the library was 80% based on approximately 50 wells assayed by HPLC (Figure 2A). The macroscopic size of the beads (600 μm diameter, dry) permitted their physical manipulation as individual sequences, i.e., one compound per well [18]. The amount of synthetic material on each bead allowed for dye binding characterization at high peptoid concentrations, HPLC analysis, and efficient MS/MS sequencing. Therefore, a single sequence could be assayed for self-assembly and identified without resorting to laborious library deconvolution approaches.

A portion of the library (3456 beads) was cleaved and assayed for 1,8-ANS binding. The 1,8-ANS fluorescence values at 460 nm for the library ranged from 2,900 to 39,000 units with a mean value of 6,010 (Figure 2B) and a standard deviation of 3,550. A total of 88 compounds had values that were three standard deviations above the mean value and were considered "hit" sequences. More than 80% of the total sequences exhibited fluorescence below 7000 units. From the group exhibiting highest fluorescence (Figure 2B, inset), eight compounds were selected for MS/MS sequencing (labeled **1–8**). Three sequences were selected at random from the region with fluorescence intensity below 7000 as negative control compounds (**9–11**).

Tandem electrospray mass spectrometry was used to sequence the unknown variable regions of the selected peptoids. The correct parent ion was identified by finding a triple-charged ion within the appropriate mass range for the library (molecular weight 2373.6–2962.4 Da). Using the negative ion mode, the MS/MS collision-induced dissociation (CID) spectrum showed predominantly C-terminal (Y type) cleavage products (e.g., sequence **4**, Figure 3). Interestingly, the tertiary backbone amide of the peptoid cleaved preferentially to the secondary amide bond found in some of the side chains. This allowed the side chains within the variable regions to be identified by simply determining the change in mass between distinct peaks on the CID spectrum and

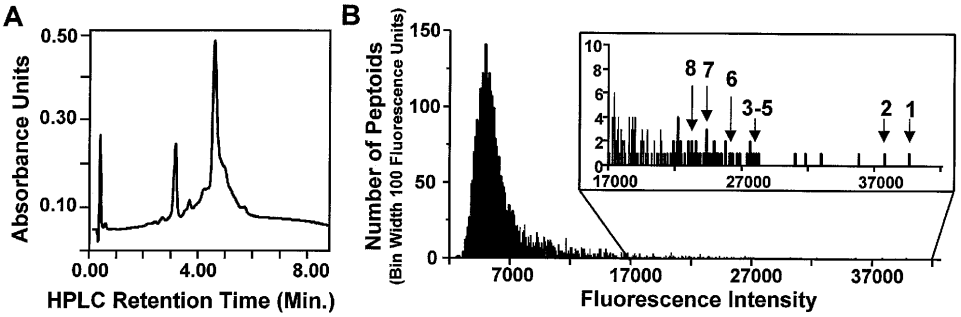

Figure 2. Single-Bead Library Characterization

(A) The analytical reverse-phase HPLC (C_4) trace of a typical crude single-bead cleavage; 10% of the cleaved material was injected after the 1,8-ANS binding assay.

(B) Peptoid sequences grouped by fluorescence intensity into bins of width 100 units. The inset is a magnification of the top 2.5% highest fluorescing sequences. Numbers represent the compounds that were sequenced by MS/MS and characterized further as individual compounds.

comparing them to known side chain masses. The summation of the predicted sequences agreed with the observed parent ions. The 1,8-ANS binding peptoids (Figure 4) shared some distinguishing sequence features. All of the sequences contained hydrophobic side chains with chiral α-methyl substitutions. However, the most common hydrophobic residue, the diphenethyl side chain, is achiral. This side chain is the most hydrophobic residue in the library as estimated by calculated log P values [19] and was found at a variety of positions along the hydrophobic face. We suspect that the prevalence of aromatic side chains may promote 1,8-ANS binding through favorable π-π interactions. It appears that a combination of hydrophobic aromatic and chiral side chains may be required for activity and self-assembly. There were no clear trends observed in the placement of the ionic side chains.

The identified active sequences were resynthesized and purified by preparative HPLC. As expected, sequences **1–8** all exhibited increasing 1,8-ANS fluorescence with increasing peptoid concentration (Figure 5), confirming that the peptoid sequences identified in the library bound the dye. The 1,8-ANS binding isotherms for sequences **1–6** and **8** were noncooperative with Hill coefficients between 1.2 and 1.3 $\pm$ 0.1. The binding isotherm for sequence **7** exhibited a Hill coefficient of 1.6 $\pm$ 0.2, indicative of a weakly cooperative binding event. In contrast, the control sequences **9–11** induced little 1,8-ANS fluorescence over the same range of peptoid concentration.

1,8-ANS binding indicates the presence of a hydrophobic core but reveals little about the assembly size. To assess the oligomerization state of the peptoids, the apparent molecular weight was investigated by size exclusion chromatography (Table 1). The retention times were compared to known protein standards in phosphate-buffered saline (PBS). Under these conditions, sequences **1–8** formed associating species ranging in

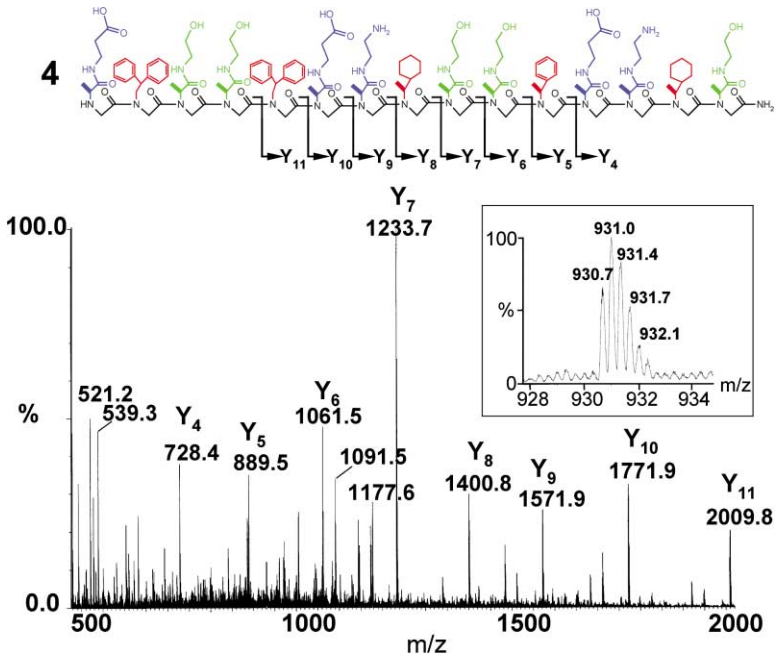

Figure 3. MS/MS Analysis of Sequence **4**

Collision-induced dissociation (CID) spectrum of the triple-charged parent ion of mass 931 (inset) observed in the nano-ESI spectrum. The negative Y ion series are annotated.

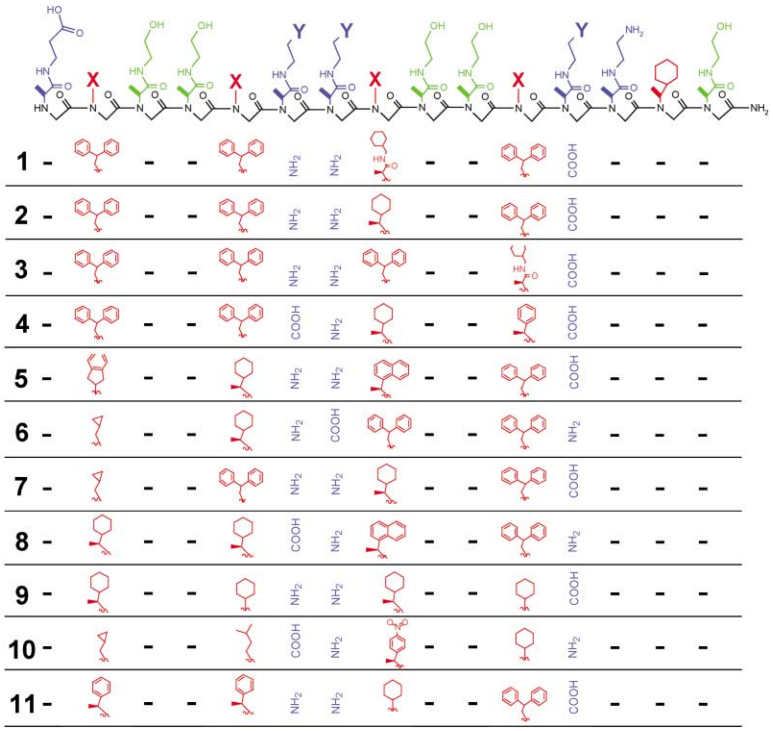

Figure 4. Sequenced Library Actives and Selected Controls

The sequences identified by MS/MS of eight 1,8-ANS binding sequences (**1–8**) and three nonbinding sequences (**9–11**) isolated from the library.

oligomeric state from dimers to tetramers in equilibrium with the monomeric species. The control sequences **9–11** exhibited limited assembly and ran roughly as their theoretical monomeric molecular weights.

Sequences **4** and **10** were selected for evaluation by sedimentation equilibrium analytical ultracentrifugation and for more thorough investigation of 1,8-ANS binding. Sedimentation equilibrium analysis showed sequence **4** self-associates in a concentration-dependent manner (Figure 6A). The data at different concentrations and rotor speeds fit best to a monomer-dimer-tetramer equilibrium model with a monomer to dimer K_d of 4.28×10^{-5} M and a dimer to tetramer K_d of 1.35×10^{-4} M (Figure 6C). The estimated dissociation constants are consistent with the 1,8-ANS binding as a function of peptoid concentration shown in Figure 5, with a tetrameric species binding 1,8-ANS. The sedimentation equilibrium data for the negative control (sequence **10**) fit best to monomer-dimer equilibrium model (Figure 6B), exhibiting some association at higher concentrations with a K_d of 4.89×10^{-4} M (Figure 6D). The stoichiometry of dye binding of 1,8-ANS was assessed by titrating ANS into a fixed concentration of peptoid (1.0 mM). 1,8-ANS bound to sequence **4** with a K_d of 181 $\pm$ 19 μM and a stoichiometry of one dye to two peptoid molecules. Sequence **10** exhibited little 1,8-ANS binding over the same concentration range. Taken together, the data

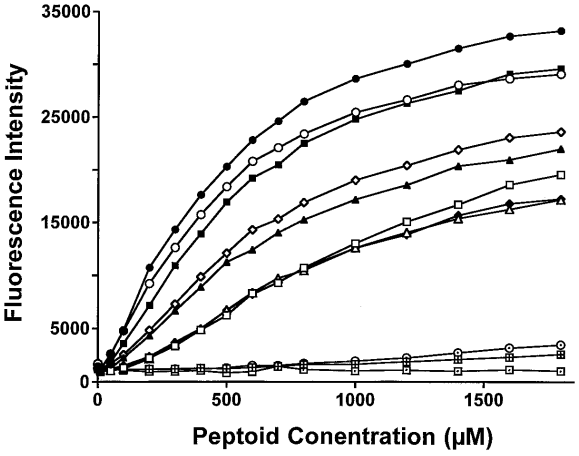

Figure 5. Individual Peptoid Characterization

1,8-ANS fluorescence emission at 460 nm as a function of peptoid concentration (based on dry weight plus appropriate counter ions) in PBS (pH 7.4) while 1,8-ANS is held constant at 50 μM. Sequences are indicated by the following symbols: **1**, filled circle; **2**, open circle; **3**, filled square; **4**, open square; **5**, filled triangle; **6**, open triangle; **7**, filled diamond; **8**, open diamond; **9**, open circle with dot; **10**, squared cross; and **11**, open square with dot.

Table 1. Size Exclusion Chromatography Data

Peptoid	Monomer Mol. Wt.	Assembly Mol. Wt.	Degree of Assembly
1	2893	11,377	3.9
2	2836	10,304	3.6
3	2895	9,654	3.3
4	2791	8,693	3.1
5	2748	7,273	2.6
6	2712	10,660	3.9
7	2712	6,872	2.5
8	2741	7,697	2.8
9	2572	3,720	1.4[a]
10	2543	3,999	1.6[a]
11	2658	3,273	1.2[a]

[a] Determined using the Superdex Peptide Column

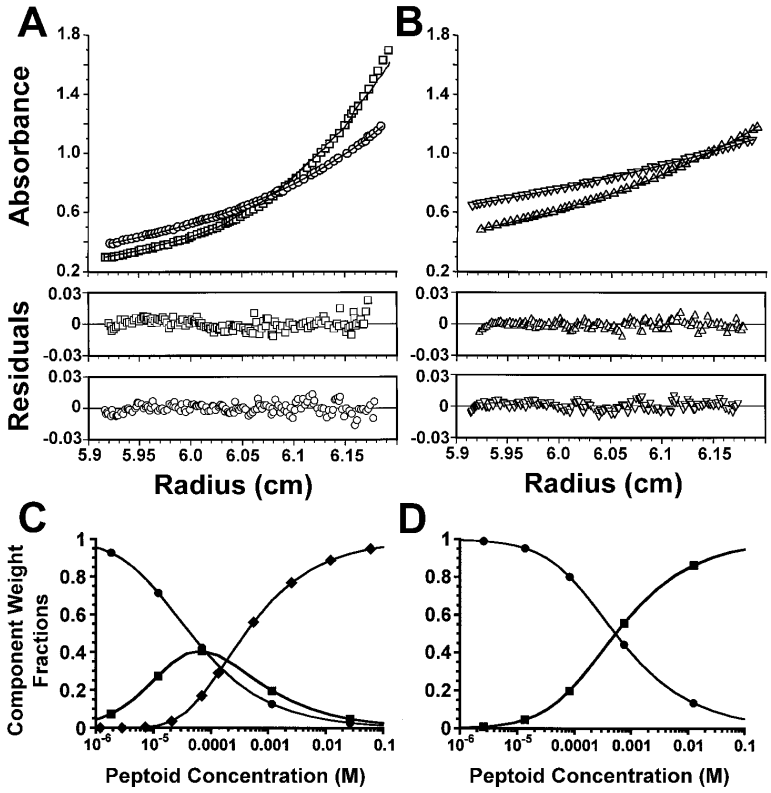

Figure 6. Sedimentation Equilibrium Analytical Ultracentrifugation

(A) The concentration distribution as a function of radial position of sequence **4** at (0.92 mM, 270 nm) at 40,000 rpm (open square) and (1.0 mM) 30,0000 rpm (open circle).

(B) The concentration distribution as a function of radial position of sequence **10** (1.0 mM, 310 nm) at 40,000 rpm (open triangle) and 30,0000 rpm (open inverted triangle). Residuals below show the fit of a monomer-dimer-tetramer model for sequence **4** and a monomer-dimer model for sequence **10**. The calculated percentages of monomer (filled circle), dimer (filled square), and tetramer (filled diamond) as a function of concentration for sequence **4** (C) and sequence **10** (D) based on the calculated association constants.

suggests that the association of four or more peptoid sequences into an assembly is required for efficient dye binding. Although the data for sequence **4** fit best to a monomer-dimer-tetramer model, the existence of other trace multimeric species at higher concentration cannot be ruled out by this method.

Circular dichroism has been used as a convenient low-resolution spectroscopic probe of secondary structure in proteins and has been adapted to study polypeptoids [20, 16]. The self-assembling sequences (**1–8**) exhibited a qualitatively different CD spectrum to that of the monomeric sequences (**9–11**). Sequences **1–8** had a peak at 208 nm and minima at 220 or 225 nm (Figure 7A), which were less pronounced in sequences **9–11** (Figure 7B). There was no discernable change in CD signal for the multimeric sequences or the monomeric sequences as the concentration of peptoid was increased from 0.05 mM to 1.5 mM. Sequences **1–8** exhibited a more pronounced change in CD signature as a function of temperature (e.g., sequence **4**, Figure 7C) but exhibited little cooperative unfolding. From the biophysical data, we conclude that sequences **1–8** exhibit secondary structure and collapse into minimal aggregates due to the hydrophobic effect, an initial step in protein tertiary structure formation.

Only 2.5% of the total number of sequences assayed in the library displayed significant ($>3\sigma$) 1,8-ANS binding. Biophysical characterization of the best binding se-

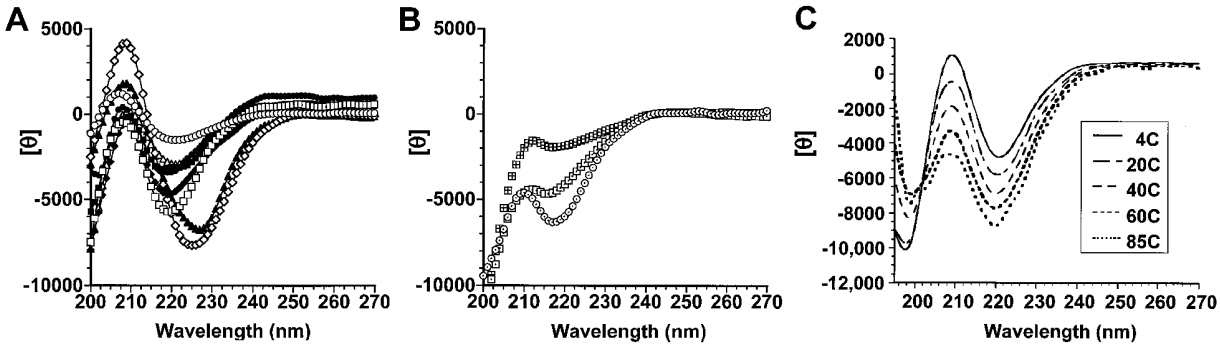

Figure 7. Peptoid Circular Dichroism Spectra

(A) The spectra for sequences **1–8** and (B) sequences **9–11**. Data are expressed in mean residue ellipticity ([θ], deg·cm^2/dmol) based on the number of residues.

(C) CD temperature denaturation of sequence **4**. Thermal hysteresis was not observed.

quences indicated that they self-associate to form folded multimeric structures under physiological conditions. However, there was little evidence of cooperativity, a hallmark of protein folding. Since monomeric peptoid helices are quite stable [20], the additional stabilization energy associated with helix bundle formation is likely to be modest. We also expect that there are many approximately iso-energetic states that are folded. To create a cooperative transition, one distinct folded structure must be substantially more stable than the other plausible assemblies or folded states. The introduction of helix-destabilizing achiral residues, the linking of helices, and the use of heteromultimeric sequences to create unique packing opportunities in the hydrophobic interior may widen the energetic gap between the desired folded state and competing states, increasing the cooperativity of the folding transition.

In fact, the progression from a molten self-associating helical sequence to a single chain folded native structure is well documented in the work of DeGrado and coworkers [21]. DeGrado and Eisenberg created a partially folded four-helix bundle using a short peptide sequence with a high helical propensity and an amphiphilic pattern [22]. The stability of the peptide assembly was improved by linking two helices together [23]. With a structural scaffold in hand, sequence effects on helix formation, helix termination, and loop influence were investigated. Later, the conformational specificity was restricted to a more native-like state through the variation of interior hydrophobic and polar interfacial residues [24, 25]. Taken together, this led to the creation of a de novo designed protein with physical properties indistinguishable from those of natural protein structures [26]. A number of researchers have used similar iterative design strategies to create a number of de novo folded proteins [27–34].

The factors that influence folding and stability are likely to be the same for abiological and biological polymers [35]. However, the precise structural and sequence-specific features of peptoids will have to be investigated in a similar manner. Undoubtedly, secondary structure capping, side chain influence on conformation, hydrophobic side chain packing, and loop flexibility will dictate folding and stability of a nonnatural structure. It is also reasonable to believe that the rules that govern peptoid folding and structure could be determined more easily than for polypeptides. For example, chiral peptoids appear to form one repeating helical structure that is largely dictated by steric repulsions between the backbone and the side chain chirality α to the backbone nitrogen [36]. Moreover, the lack of backbone hydrogen bond donors simplifies the intrinsic main chain conformational preferences. Thus, the peptoid scaffold may provide a simpler template to identify the rules for the design of functional folded heteropolymeric macromolecules.

The peptoid architecture is a cost-effective and sequentially distinct variation of biological polymers. While they have many characteristics in common with peptides, polypeptoids may circumvent many of nature's defenses as they are resistant to proteases [37]. This improves their biological half-life and apparently helps them to evade part of the immune response. Polypeptoids are thermally stable and likely have unique membrane permeability. These biological properties were exploited in developing peptoids that have been utilized in nucleic acid delivery [38] as a potent and selective SH3 analog [39] and as a cellular entry vehicle [40].

Significance

Because there is little precedent for the de novo design and synthesis of a completely synthetic macromolecule of defined tertiary structure [8], we approached this problem by mimicking nature's process of natural selection. Sequence variation and selection for function were used to identify amphiphilic peptoid sequences that bound a ligand by forming a noncovalent self-assembling macromolecular structure. With this accomplishment, a high-throughput, general approach to the discovery of novel activity was developed utilizing diverse synthetic libraries, individual compound activity assays, and a means of direct compound identification. As the synthetic tools for peptoid heteropolymer synthesis have become more efficient in recent years, large libraries of protein-like sequences are now attainable. Rather than attempt to predict the folding of each sequence variant, we chose to screen directly for function. Our initial success shows that helical peptoids can self-associate and begin to form structures analogous to those found in nature. With further modifications and refinement in structure design, it is reasonable to believe that a stable continuous chain polypeptoid nanostructure could be made. This type of architecture would be useful in the design of functional heteropolymers that bind to nucleic acids, small molecules, or protein interfaces.

Experimental Procedures

Library Synthesis and Characterization

Solvents and reagents were obtained from commercial sources and used without further purification. The alanine *N'*-substituted amide submonomers were prepared in high yield in two steps from Cbz-protected L-alanine following the procedure of Bodanszky [41]. A detailed monomer synthesis procedure is provided as supplemental material. Reactive side chains functionalities were protected with the appropriate acid labile protecting groups. The hydroxyethyl group was protected as the triisopropylsilylether, the aminoethyl group was protected as the *t*-butyl carbamate, and the carboxyethyl group was protected as the *t*-butyl ester. The precursor amines, mono-Boc-ethylenediamine and 2-[(triisopropylsilyl)oxy]ethylamine, were prepared in one step [42].

The combinatorial macrobead library was prepared on 1.2 g (100 mg/bin) of 600 μm diameter polystirene beads (Rink amide resin, 0.75 mmol/g, Polymer Labs Amherst, MA). The mix-and-split library was synthesized using a robotic synthesizer [43]. Stepwise peptoid synthesis consists of two steps. First, bromoacetic acid is coupled using carbodiimide in DMF, and then the bromide is displaced with an amine (1.0–2.0 M) in NMP. Prior to use in the library, the coupling efficiency for each amine submonomer was evaluated in a pentamer sequence under standard conditions [19]. The following minor changes were made to ensure uniform coupling yields during library synthesis: two successive 15 min bromoacetylation steps were performed, followed by a 60 min displacement step. The reaction time for the last five displacement steps was increased to 90 min. Each resin distribution and recombination step was repeated three times to insure complete transfer.

Each bin (12 total) of 100 mg resin identified by the N-terminal hydrophobic side chain was allowed to swell overnight in dichloro-

ethane (DCE). A robotic bead distributor was used to place one bead per well into a 96-well plate. Three plates per bin were distributed. The peptoid was cleaved from the single bead, and the side chain was deprotected in 30:67:2:1 trifluoroacetic acid (TFA)/DCE/H_2O/triethylsilane (v/v) for 14 hr. The cleavage cocktail was removed by centrifugation in vacuo. The peptoid product was resuspended and extracted from the bead with 100 μl 10:89:1 acetic acid/acetonitrile/H_2O and transferred to a new plate. The extraction solution was then removed by centrifugation in vacuo and the peptoid was resuspended in PBS. The library purity was evaluated by reverse phase analytical HPLC on a Waters 2690 system with a photodiode array detector. Ten microliters of the total volume per well was injected onto a C_4 Column (Duragel G, 3 μm, 300 A, 0.2 × 5.0 cm) using a linear gradient from 5% to 95% solvent B in solvent A (solvent A, water + 0.1 % TFA [v/v]; solvent B, acetonitrile + 0.095% TFA [v/v]) at 1.0 ml/min and 60°C over 10 min. The peptoid molecular weight was verified by liquid chromatograph/mass spectrometry (LCMS) using a Hewlett Packard 1100 electrospray system in the positive mode with a 125V cone voltage.

Self-Assembly Assay

The PBS solution of crude peptoid from the single-bead cleavage was solubilized in 90 μl PBS (pH 7.4). The pH was verified with pH paper (2–3 wells per plate). To each well, 10 μl of 1,8-ANS stock ($\epsilon_{350} = 4.95 \times 10^{-3}$ l/mol-cm) solution was added to a final concentration of 50 μM 1,8-ANS. The fluorescence emission was measured at room temperature at 460 nm using a Wallac Victor 1420 multilabel counter 96-well plate reader. The excitation wavelength was 370 nm with a bandwidth filter of 10 nm. Data was collected for 0.1 sec/well.

MS/MS Sequencing

From the desired well, 3 μl of solution was loaded onto an equilibrated Millipore P10 C4 ZipTip. The tip was then washed with H_2O, and the peptoid was eluted with 2–5 μl of 70/29/1 acetonitrile/H_2O/formic acid (v/v). The eluted solution was then diluted with 10 μl methanol to increase sample viscosity and injected directly into the MicroMass Q-TOF mass spectrometer using a nanoelectrospray source. The MS/MS product ion spectra were obtained in the triple-quadrupole negative scan mode by selectively introducing the M+3/z3 precursor ion into the collision cell and observing the product ion distribution in the third quadrupole. The CID product ion spectra were collected from 500–2500 with an increment size 0.1 amu and a dwell time of 0.2 ms.

Individual Peptoid Synthesis and Characterization

Single peptoid compounds were synthesized and cleaved from the resin following protocols outlined above. The crude peptoid was precipitated by dropwise addition of the cleavage mixture to cold diethyl ether. The precipitant was washed with cold diethyl ether (2 × 50 ml) and lyophilized from water. The synthetic purity was evaluated by analytical reverse-phase HPLC, and the compounds were verified by LC/MS as described above. Peptoids were purified by reverse-phase preparative HPLC on a Rainin Dynamax SD-200 system using a Duragel HS C4 Column (50 μm, 300 A, 50 × 20 mm) at 50°C with a linear gradient from 19% to 45% solvent B into solvent A over 15 min at 40 ml/min to greater than 95% purity. After lyophilization, the purified product was desalted using a Pharmacia LCC-500 fast desalting column at 1.5 ml/min and lyophilized. 1,8-ANS binding experiments on individual purified peptoids were performed as described above. All binding isotherms were fit to the Hill equation using the nonlinear least-squares method found in the graphing software Microcal™ Origin™ (Northampton, MA).

Size Exclusion Chromatography

Fifty microliters of a 0.01 M peptoid solution was injected onto either a Superose 12 10/30 or Superdex Peptide 10/30 FPLC column using a Waters 2690 system with a photodiode array detector in PBS (pH 7.4) at 0.5 ml/min and 23°C. There was a 10-fold dilution of the sample upon injection. A log (molecular weight) versus retention time standard curve was prepared with molecular weight standards (0.1 mg/ml); ovalbumin, myoglobin, cytochrome C, insulin, insulin B chain, and cyanocobalamin. Peptoid molecular weights were interpolated from the standard curves.

Sedimentation Equilibrium Analytical Ultracentrifugation

The experiment was preformed on a Beckman Model XL-I analytical ultracentrifuge with a 4-sample An-60 Ti rotor using a 6-channel 1.2 mm column cell assembly. Each peptoid concentration (1.0, 0.5, 0.25, and 0.05 mM) was run at 4°C in PBS (pH 7.4) at both 30,000 and 40,000 rpm. The absorbance was recorded at wavelengths from 230 to 330 depending on the concentration and side chain chromophores. The data are a summation of ten scans with an increment width of 0.001 cm collected after equilibrium is achieved. The partial specific volume of the peptoid was estimated based on similar amino acids using the program SEDINTERP [44]. A global fit of the data using a variety of different self-association models at different concentrations and rotor speeds was performed using the nonlinear least-squares fitting program NONLIN [45].

Circular Dichroism Spectroscopy

The circular dichroism spectra were recorded on a Jasco model 720 spectropolarimeter equipped with a Peltier temperature control unit. Spectra of peptoids in 0.05 M phosphate buffer at 23°C were collected in a 0.01 or 0.1 cm path length quartz cell with an average of four scans. Data are expressed in mean residue ellipticity ([θ], deg·cm^2/dmol) based the number of residues. For CD Temperature denaturation, the sample was allowed to equilibrate for 15 min between temperature increments.

Supplemental Material

A detailed synthetic procedure for the synthesis of the propanamide monomer is available through the *Chemistry & Biology* Production Department. Please write to chembiol@cell.com for a pdf.

Acknowledgments

This work was supported by the National Institutes of Health (GM-33900 and a postdoctoral fellowship for T.S.B. [GM-20501]) and Chiron Technologies. We thank Dr. Ying Rong Yang, Professor Howard Schachman, and Professor R. Dyche Mullins for help with the analytical ultracentrifugation.

Received: January 29, 2002
Revised: March 18, 2002
Accepted: March 22, 2002

References

1. Richardson, J.S. (1981). The anatomy and taxonomy of protein structure. Adv. Protein Chem. *34*, 167–339.
2. Hill, D.J., Mio, M.J., Prince, R.B., Hughes, T.S., and Moore, J.S. (2001). A field guide to foldamers. Chem. Rev. *101*, 3893–4012.
3. Cheng, R.P., Gellman, S.H., and DeGrado, W.F. (2001). Beta-peptides: from structure to function. Chem. Rev. *101*, 3219–3232.
4. Prins, L.J., Reinhoudt, D.N., and Timmerman, P. (2001). Noncovalent synthesis using hydrogen bonding. Angew. Chem. Int. Ed. Engl. *40*, 2382–2426.
5. Barron, A.E., and Zuckermann, R.N. (1999). Bioinspired polymeric materials: in-between proteins and plastics. Curr. Opin. Chem. Biol. *3*, 681–687.
6. Stigers, K.D., Soth, M.J., and Nowick, J.S. (1999). Designed molecules that fold to mimic protein secondary structures. Curr. Opin. Chem. Biol. *3*, 714–723.
7. Gellman, S.H. (1998). Foldamers: a manifesto. Acc. Chem. Res. *31*, 173–180.
8. Raguse, T.L., Lai, J.R., LePlae, P.R., and Gellman, S.H. (2001). Toward β-peptide tertiary structure: self-association of an amphiphilic 14-helix in aqueous solution. Org. Lett. *3*, 3963–3966.
9. Zuckermann, R.N., Kerr, J.M., Kent, S.B.H., and Moos, W.H. (1992). Efficient method for the preparation of peptoids [oligo(*N*-substituted glycine)] by submonomer solid-phase synthesis. J. Am. Chem. Soc. *114*, 10646–10647.
10. Armand, P., Kirshenbaum, K., Goldsmith, R.A., Farr-Jones, S.,

Barron, A.E., Truong, K.T., Dill, K.A., Mierke, D.F., Cohen, F.E., Zuckermann, R.N., et al. (1998). NMR determination of the major solution conformation of a peptoid pentamer with chiral side chains. Proc. Natl. Acad. Sci. USA *95*, 4309–4314.

11. Beausoleil, E., Truong, K.T.V., Kirshenbaum, K., and Zuckermann, R.N. (2001). Influences of monomer structural elements in hydrophilic peptoids. In Innovations and Perspectives in Solid Phase Synthesis and Combinatorial Libraries: Peptides, Proteins, and Nucleic Acids, R. Epton, ed. (Kingswinford, UK: Mayflower Scientific Press), pp. 239–242.
12. Moffet, D.A., and Hecht, M.H. (2001). De novo proteins from combinatorial libraries. Chem. Rev. *101*, 3191–3203.
13. Schonbrunn, E., Eschenburg, S., Luger, K., Kabsch, W., and Amrhein, N. (2000). Structural basis for the interaction of fluorescence probe 8-anilino-1-naphthalene sulfonate (ANS) with the antibiotic target MurA. Proc. Natl. Acad. Sci. USA *97*, 6345–6349.
14. Ptitsyn, O.B., Pain, R.H., Semisotnov, G.V., Zerovnik, E., and Razgulyaev, O.L. (1990). Evidence for a molten globule state as a general intermediate in protein folding. FEBS Lett. *262*, 20–24.
15. Kane, C.D., and Bernlohr, D.A. (1996). A simple assay for intracellular lipid-binding proteins using displacement of 1-anilinonaphthalene 8-sulfonic acid. Anal. Biochem. *233*, 197–204.
16. Wu, C.W., Sanborn, T.J., Huang, K., Zuckermann, R.N., and Barron, A.E. (2001). Peptoid oligomers with α-chiral, aromatic side chains: sequence requirements for the formation of stable peptoid helices. J. Am. Chem. Soc. *123*, 2958–2963.
17. Presnell, S.R., and Cohen, F.E. (1989). Topological distribution of four-α-helix bundles. Proc. Natl. Acad. Sci. USA *86*, 6592–6598.
18. Blackwell, H.E., Peres, L., Stavenger, R.A., Tallarico, J.A., Eatough, E.C., Foley, M.A., and Schreiber, S.L. (2001). A one-bead, one-stock solution approach to chemical genetics: part 1. Chem. Biol. *8*, 1167–1182.
19. Lipinski, C.A., Lombardo, F., Dominy, B.W., and Feeney, P.J. (1997). Experimental and computational approaches to estimate solubility and permeability in drug discovery and development settings. Adv. Drug Deliv. Rev. *23*, 3–26.
20. Kirshenbaum, K., Barron, A.E., Goldsmith, R.A., Armand, P., Bradley, E.K., Truong, K.T., Dill, K.A., Cohen, F.E., and Zuckermann, R.N. (1998). Sequence-specific polypeptoids: a diverse family of heteropolymers with stable secondary structure. Proc. Natl. Acad. Sci. USA *95*, 4303–4308.
21. Hill, R.B., Raleigh, D.P., Lombardi, A., and DeGrado, W.F. (2000). *De novo* design of helical bundles as models for understanding protein folding and function. Acc. Chem. Res. *33*, 175–178.
22. Eisenberg, D., Wilcox, W., Eshita, S.M., Pryciak, P.M., Ho, S.P., and DeGrado, W.F. (1986). The design, synthesis, and characterization of an alpha-helical peptide. Proteins *1*, 16–22.
23. Ho, S.P., and DeGrado, W.F. (1987). Design of a 4-helix bundle protein: synthesis of peptides which self-associate into a helical protein. J. Am. Chem. Soc. *109*, 6751–6758.
24. Raleigh, D.P., and DeGrado, W.F. (1992). A *de novo* designed protein shows a thermally induced transition from native to a molten globule-like state. J. Am. Chem. Soc. *114*, 10079–10081.
25. Hill, R.B., Hong, J., and DeGrado, W.F. (2000). Hydrogen bonded cluster can specify the native state of a protein. J. Am. Chem. Soc. *122*, 746–747.
26. Hill, R.B., and DeGrado, W.F. (1998). Solution structure of α_2D, a nativelike *de novo* designed protein. J. Am. Chem. Soc. *120*, 1138–1145.
27. Baltzer, L., Nilsson, H., and Nilsson, J. (2001). *De novo* design of proteins—what are the rules? Chem. Rev. *101*, 3153–3163.
28. Imperiali, B., and Ottesen, J.J. (1999). Uniquely folded miniprotein motifs. J. Pept. Res. *54*, 177–184.
29. Michlatcher, C., and Chmielewski, J. (1999). Helical peptide and protein design. Curr. Opin. Chem. Biol. *3*, 724–729.
30. Schafmeister, C.E., and Stroud, R.M. (1998). Helical protein design. Curr. Opin. Chem. Biotechnol. *4*, 350–353.
31. Kohn, W.D., and Hodges, R.S. (1998). Alpha-helical protein assembly motiffs. Trends Biotechnol. *16*, 379–389.
32. Gellman, S.H. (1998). Minimal model systems for beta sheet secondary structure in proteins. Curr. Opin. Chem. Biotechnol. *2*, 717–725.
33. Lacroix, E., Kortemme, T., Lopez de la Paz, M., and Serrano, L. (1999). The design of linear peptides that fold as monomeric beta-sheet structures. Curr. Opin. Struct. Biol. *4*, 487–493.
34. Beasley, J.R., and Hecht, M.H. (1997). Protein design: the choice of *de novo* sequences. J. Biol. Chem. *272*, 2031–2034.
35. Dill, K.A. (1990). Dominant forces in protein folding. Biochemistry *29*, 7133–7155.
36. Armand, P., Kirshenbaum, K., Falicov, A., Dunbrack, R.L., Jr., Dill, K.A., Zuckermann, R.N., and Cohen, F.E. (1997). Chiral *N*-substituted glycines can form stable helical conformations. Fold. Des. *2*, 369–375.
37. Miller, S.M., Simon, R.J., Ng, S., Zuckermann, R.N., Kerr, M.J., and Moos, W.H. (1995). Comparison of the proteolytic susceptibilities of homologous L-amino acid, D-amino acid, and *N*-substituted glycine peptide and peptoid oligomers. Drug Dev. Res. *35*, 20–32.
38. Huang, C.Y., Uno, T., Murphy, J.E., Lee, S., Hamer, J.D., Escobedo, J.A., Cohen, F.E., Radhakrishnan, R., Dwarki, V., and Zuckermann, R.N. (1998). Lipitoids—novel cationic lipids for cellular delivery of plasmid DNA *in vitro*. Chem. Biol. *5*, 345–354.
39. Nguyen, J.T., Turck, C.W., Cohen, F.E., Zuckermann, R.N., and Lim, W.A. (1998). Exploiting the basis of proline recognition by SH3 and WW domains: design of *N*-substituted inhibitors. Science *282*, 2088–2092.
40. Wender, P.A., Mitchell, D.J., Pattabiraman, K., Pelkey, E.T., Steinman, L., and Rothbard, J.B. (2000). The design, synthesis, and evaluation of molecules that enable or enhance cellular uptake: peptoid molecular transporters. Proc. Natl. Acad. Sci. USA *97*, 13003–13008.
41. Bodanszky, M. (1984). Activation and coupling. In The Practice of Peptide Synthesis, K. Hafner, J.-M. Lehn, C.W. Rees, F.R.S. Hoffmann, P.V. Raque-Schleyer, B.M. Trost, and R. Zahradnik, eds. (Berlin: Springer-Verlag), pp. 109–110.
42. Zuckermann, R.N., Martin, E.J., Spellmeyer, D.C., Stauber, G.B., Shoemaker, K.R., Kerr, J.M., Figliozzi, G.M., Goff, D.A., Siani, M.A., Simon, R.J., et al. (1992). Discovery of nanomolar ligands for 7-transmembrane G-protein-coupled receptors from a diverse *N*-(substituted)glycine peptoid library. J. Med. Chem. *37*, 2678–2685.
43. Zuckermann, R.N., Kerr, J.M., Siani, M.A., and Banville, S.C. (1992). Design, construction, and application of a fully automated equimolar peptide mixture synthesizer. Int. J. Pept. Protein Res. *40*, 497–506.
44. Laue, T., Shaw, B.D., Ridgeway, T.M., and Pelletier, S.L. (1992). Computer-aided interpretation of analytical sedimentation data for proteins. In Analytical Ultracentrifugation in Biochemistry and Polymer Science, S.E. Harding, ed. (Cambridge, UK: Royal Society of Chemistry), pp. 90–125.
45. Johnson, M.L., Correia, J.J., Yphantis, D.A., and Halvorson, H.R. (1981). Analysis of data from the analytical ultracentrifuge by nonlinear least-squares techniques. Biophys. J. *36*, 575–587.